Nonideal *J-V* characteristics and interface states of an *a*-Si:H Schottky barrier

Keiji Maeda and Ikuro Umezu
Faculty of Industrial Science and Technology, Science University of Tokyo, Noda, Chiba 278, Japan

Hideaki Ikoma and Takahiro Yoshimura
Faculty of Science and Technology, Science University of Tokyo, Noda, Chiba 278, Japan

(Received 6 March 1990; accepted for publication 30 May 1990)

A new theory is developed for nonideal *J-V* characteristics of Schottky barriers with an interfacial layer. This theory is based on the model that nonideal characteristics are due to changes of population in the interface states under applied bias and accompanying changes of the barrier height. The population in the interface states is expressed by the Fermi level, which can be determined by analyzing experimental results. The *J-V* characteristics are obtained from the flow of carriers into and out of the interface. Tunneling through the interfacial layer constitutes the bottleneck for the carrier flow. Under forward bias, the carrier concentration n_s at the interface is proved to be in thermal equilibrium with the bulk. Under reverse bias, n_s is in local thermal equilibrium with the interface states. This theory is applied to an undoped *a*-Si:H Schottky barrier without introducing any ambiguous quantities. The experimental ideality factor, its dependence on temperature and voltage, and current density are quantitatively explained. By analyzing experimental results, the following behaviors are disclosed. The Fermi level of the interface states is significantly lower than the bulk Fermi level at low forward bias, but it approaches the bulk Fermi level with increasing forward-bias voltage. As for the reverse characteristics, the decrease of the barrier height is proportional to $\sqrt{V}$ in the present sample for applied voltage V. For electrons in the interface states, the probability of tunnel transition to the metal is small compared with that of communication with the conduction band.

I. INTRODUCTION

The Schottky barrier diode is one of the most simple semiconductor devices of fundamental importance. However, its *J-V* characteristics usually cannot be described by the theory of ideal metal-semiconductor contact. While the thermionic emission theory and the diffusion theory are based on different current transport mechanisms, both theories give nearly the same *J-V* characteristics.[1-3] Additional carrier transport mechanisms to explain the excess current have been considered, such as tunneling current through the barrier and generation-recombination current in the depletion region.[1-3] In many studies, however, the excess current has been attributed to uncertain edge leakage current at the contact periphery or interface current due to traps at the metal-semiconductor interface.[1-3]

Under conditions of Schottky barrier formation, the semiconductor surface is considered to be covered ordinarily with a thin layer of native oxide. At the boundary between the semiconductor and the oxide layer, the presence of interface electronic states is expected with a high state density in the forbidden energy gap. This interfacial layer model of the actual Schottky barrier successfully explains the dependence of the Schottky barrier height on the metal work functions.[1,2,4] This explanation is based on the thermal equilibrium conditions at zero applied bias. In this case, the Fermi levels are the same across the metal-semiconductor contact. However, when a bias voltage is applied to the Schottky barrier, the Fermi levels differ by that amount across the metal-semiconductor contact. The Fermi level of the interface states should be between these two Fermi levels. It is considered to be varied with the applied bias. Depending on the position of the Fermi level of the interface states, the space charge at the interface changes and the barrier height is also changed. Although this change of the barrier height with applied bias is complicated, it is considered to be similar by nature to the change of barrier height with the metal work functions.

According to the ordinary Schottky barrier theory, the semiconductor makes intimate contact with the metal.[1-3] The thermionic emission theory considers that the actual process of electron emission into the metal is the bottleneck for the carrier flow. On the other hand, the diffusion theory considers that the transport of electrons through the depletion region constitutes the bottleneck for the carrier flow. The interfacial layer has been assumed to be thin enough for the electron tunneling to occur with high transmission coefficient. However, the transmission coefficient of thin insulating layers of several atomic layer thick is estimated to be small compared to unity.[5] Therefore, for Schottky barriers with an interfacial layer which impedes the current flow, a different approach can be made. It is plausible to consider for low applied bias that there is an equilibrium of carrier flow at the interface between the tunneling electrons and drifting electrons to and from the bulk. The *J-V* characteristics can be obtained from the flow of carriers into and out of the interface. Under forward bias, the carrier concentration at the interface is expected to be approximately in thermal equilibrium with the bulk

 0021-8979/90/182858-10$03.00

even for low-mobility semiconductors. Under reverse bias, the carrier concentration at the interface decreases with reverse bias due to the increased carrier flow into the bulk. The interface states are in equilibrium with this carrier concentration. Therefore, the population in the interface states and also the barrier height are considered to be varied with reverse bias.

Up to now, few papers treated the importance of the interfacial layer and the interface states in the J-V characteristics of Schottky barrier except for the barrier height at zero bias.[1,2,4] The structure of Schottky barrier with an interfacial layer is the same as that of tunnel metal-oxide-semiconductor (MOS) diode. For the present investigation, studies of tunnel MOS diodes by Card and Rhoderick[5] are very important and suggestive. Recently, Horvath[6] extended the analysis of Card and Rhoderick[5] and evaluated the energy distribution of the interface state density from the J-V characteristics of Schottky barriers by making special assumptions on the interface states.

Since undoped hydrogenated amorphous Si, a-Si:H, is one of the low-mobility and high-resistivity n-type semiconductors and has a large field of applications, it is an appropriate material for investigating the characteristics of Schottky barriers in detail.[7]

In this paper, a new theory of J-V characteristics of the Schottky barrier with an interfacial layer is developed in Sec. II from the viewpoint stated above. The sample preparation of a-Si:H Schottky barrier is described in Sec. III. The J-V characteristics are measured at various temperatures between 30 and 150 °C in both forward and reverse directions. The observed J-V characteristics differ considerably from the ideal theory. The experimental results are analyzed quantitatively by the above interfacial layer model in Sec. IV. This analysis discloses the behavior of the interface states under the applied biases. Simplifying assumptions as well as consistency among various quantities involved in the present model are discussed in Sec. V.

II. INTERFACIAL LAYER MODEL

The interfacial layer model considers that the semiconductor and metal are separated by a thin insulating layer of thickness δ and dielectric constant ϵ_i and there are localized electronic states at the insulator-semiconductor interface.[1,4] It may be oversimplified because the interface states are represented by point charges, whereas in fact they may spread over a distance of atomic dimension.

The interfacial layer in the a-Si:H Schottky barrier consists of native oxide on the surface. The a-Si:H surface has low reactivity with oxygen because of bond saturation with hydrogen.[8] The oxide growth on the surface exposed to room ambience was found to follow a parabolic time dependence assuming constant values of the optical properties of the oxide.[9] The oxide thickness was less than 10 Å within a week. Therefore, it is reasonable that consistent values have been reported for the barrier height of the a-Si:H Schottky barrier.

In the following, an interfacial layer model is developed for the J-V characteristics of Schottky barrier. There are many possible factors influencing the J-V characteristics. However, dominant factors related to the characteristics are considered in this section. Simplifying assumptions involved in this model are discussed in Sec. V.

A. Change of barrier height

Experimentally, the dependence of the a-Si:H Schottky barrier height ϕ_B^0 at zero applied bias voltage on the metal work function ϕ_m is given by[7]

$$\phi_B^0 = 0.25\phi_m - 0.33(\mathrm{V}).$$

According to the interfacial layer model,[1,4] ϕ_B^0 is represented by

$$\phi_B^0 = \gamma(\phi_m - \chi) + (1-\gamma)[(E_g/q) - \phi_0], \tag{1}$$

where

$$\gamma = 1/[1 + (q\delta D_s)/\epsilon_i], \tag{2}$$

χ is the electron affinity, D_s is the interface state density (/eV cm^2), E_g is the band-gap energy, ϕ_0 is the neutral level of the interface states measured from the top of the valence band E_V, and q is the electronic charge.

By comparison of Eq. (1) with the experimental relation, the value of γ in an a-Si:H Schottky barrier is equal to 0.25. Although there are ambiguities for the values of δ and ϵ_i, we obtain $D_s \simeq 7\times 10^{13}$ states/eV cm^2 and $\phi_0 \simeq 0.9$ V from Eqs. (1) and (2) if we assume $\delta \simeq 10$ Å and $\epsilon_i \simeq 4\epsilon_0$, ϵ_0 being the permittivity of free space. These values are reasonable in reference to the reported values.[4,7]

When a bias voltage V is applied to the Schottky barrier, the occupation of electrons in the interface states is considered to change. The equation relating space charge in the interface states and the potential is given by

$$\phi_m + \frac{q\delta}{\epsilon_i}\left[\left(\frac{E_g}{q} - \phi_B - \phi_0\right)D_s + VD_{sb}\right] = \chi + \phi_B. \tag{3}$$

Here, VD_{sb} represents the density of the occupied interface states/cm^2 due to the applied voltage, in the same way as $(E_g/q - \phi_B - \phi_0)D_s$ represents the density of electrons in the interface states contributing to the space charge under zero bias. Other terms in Eq. (3) are the same as those in the equation used to obtain Eq. (1) without application of bias voltage,[1,4] except for ϕ_B replaces ϕ_B^0 under applied voltage. In Eq. (3), the zero-temperature approximation is used for the occupation of the interface states. VD_{sb} is related to the Fermi energy E_{Fi} of the interface states above the metal Fermi energy E_{Fm} by $(VD_{sb}/D_s) = (E_{Fi} - E_{Fm})/q$ under the applied bias V. Hereafter, the metal Fermi energy is taken as the zero level of energy, i.e., $E_{Fm} = 0$. When bias voltage is applied, both the interfacial potential V_i and the surface potential V_D change. These quantities are defined as shown in Fig. 1. In addition, the bottom of the conduction band E_c and its energy difference $q\xi$ above the Fermi energy E_{Fs} in the bulk semiconductor, $q\xi = E_c - E_{Fs}$, are also shown in Fig. 1.

Equation (3) gives the change of barrier height $\Delta\phi_B$ due to the application of the bias voltage as

$$\Delta\phi_B = \phi_B - \phi_B^0 = (1-\gamma)(D_{sb}/D_s)V. \tag{4}$$

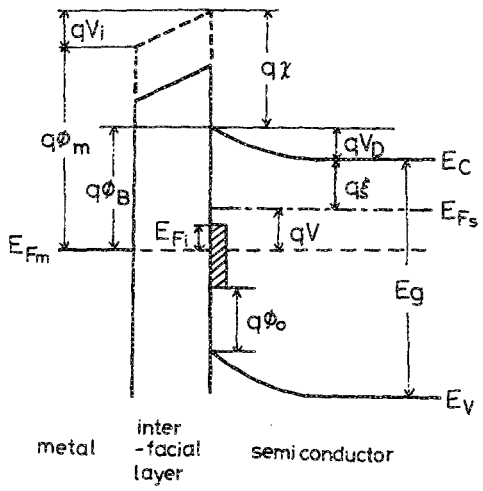

FIG. 1. Energy-band diagram of the Schottky barrier with interfacial layer under forward bias V. Various quantities in the text are defined as shown. The shaded area indicates the electron population in the interface states constituting space charge. The dashed line in the interfacial layer represents the vacuum level.

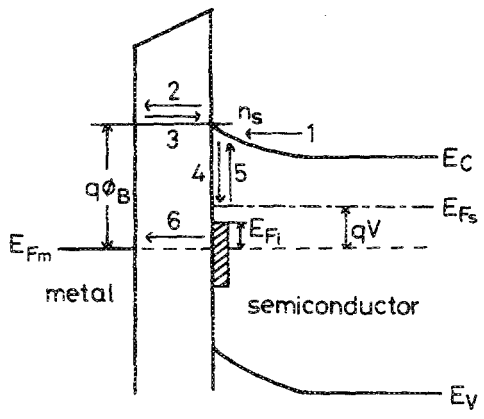

FIG. 2. Energy-band diagram of the Schottky barrier under forward bias illustrating electron flows and transitions. The shaded area indicates occupied interface states.

This change of barrier height is the cause of departure from the ideal characteristics of the Schottky barrier. Here, the image force lowering[2] of the barrier is neglected. The image force lowering is discussed in Sec. V. When a voltage V is applied, the changes of V_D and V_i are related by

$$\Delta V_D = V_D - V_D^0 = \Delta\phi_B - V$$
$$= (V/D_s)[(1-\gamma)D_{sb} - D_s] \qquad (5)$$

and $\Delta V_i = V_i - V_i^0 = \Delta\phi_B$, since $\phi_m + V_i = \chi + \phi_B$ and $\phi_B = V_D + \xi + V$ as shown in Fig. 1. Here, V_D^0 and V_i^0 stand for the values of V_D and V_i at zero bias, respectively.

The space charge in the depletion region is neglected in Eq. (3) for simplicity, because it is quite small compared with the interfacial space charge. An estimation of the relative magnitude of the space charge Q_D in the depletion region to the space charge Q_i in the interface states is made as follows. While the magnitude of V_i is the same order of V_D, the extent of the field, where V_i and V_D are applied, respectively, i.e., the interfacial layer thickness δ and the depletion width d, are different by more than two orders of magnitude; $\delta \simeq 10$ Å and $d \simeq$ several thousands of Å. The potential difference and the space charge are related by

$$V_i \simeq Q_i\delta/\epsilon_i \text{ and } V_D \simeq qN_Dd^2/2\epsilon_s = Q_Dd/2\epsilon_s,$$

where ϵ_s and N_D are the dielectric constant and the ionized donor density of the semiconductor, respectively. The ratio of the space charges is roughly given by

$$Q_D/Q_i \simeq (\epsilon_s/\epsilon_i)(2\delta/d)(V_D/V_i).$$

Here, ϵ_s and ϵ_i are of the same order of magnitude. Therefore, the space charge in the depletion region can be neglected compared to the space charge in the interface states.

The following relation should be noted in connection with Fig. 1. Since $E_g > q(\phi_0 + \phi_B)$ as shown in Sec. V and $|Q_i| \gg |Q_D|$ as shown above, the space charge in the metal $Q_m = -(Q_i + Q_D)$ is positive. Therefore, the relation $\phi_m + V_i = \chi + \phi_B$ holds as shown in Fig. 1, but not the relation $\phi_m = V_i + \chi + \phi_B$ as has been considered,[1,2] all terms being positive.

B. J-V characteristics

The J-V characteristics can be obtained from the carrier flow in terms of the carrier concentration n_s at the interface as follows: The current J due to electron flow at the interface from the semiconductor to the metal is given by

$$J = qn_s\mu\frac{d\xi}{dx}$$
$$= qP[n_s - N_m(q\phi_B)\exp(-q\phi_B/kT)]. \qquad (6)$$

Figure 2 illustrates electron flows and transitions considered in the present model. Equation (6) takes into account the drift current in semiconductor (flow 1 in Fig. 2), the tunnel current of conducting carriers from the semiconductor to metal (flow 2 in Fig. 2), and the tunnel current of conducting carriers from the metal to semiconductor (flow 3 in Fig. 2). In Eq. (6), P is the tunneling probability of the conducting electron, $N_m(q\phi_B)$ is the state density of the metal for the energy $q\phi_B$ above the Fermi level, μ is the conductivity mobility, ξ is the quasi-Fermi level in the semiconductor, kT is the thermal energy, and x is the position in the Schottky barrier. In the last expression of Eq. (6), the first term in the parenthesis corresponds to the tunnel transition from the semiconductor to metal (flow 2), and the second term corresponds to that in reverse direction (flow 3). For the forward bias, the current J and $d\xi/dx$ (flow 1) are positive. For the reverse bias, since the carriers are driven by the field in the opposite direction, J and $d\xi/dx$ are negative. The electron capture (transition 4 in Fig. 2) and thermal release (transition 5 in Fig. 2) are approximately in a detailed balance under a steady state, since the rate of the tunnel transition of electrons in the interface states to the metal (flow 6 in Fig. 2) is smaller

than other rates of competing processes (transitions 2, 4, and 5 in Fig. 2) and does not influence the J-V characteristics as discussed in Secs. IV A and V.

Equation (6) is also satisfied under the zero-bias condition, where $d\zeta/dx = 0$, $\phi_B = \phi_B^0$, and $n_s = N_c \exp(-q\phi_B^0/kT)$, N_c being the effective state density of the conduction band. Then, $N_m(q\phi_B)$ is determined to be equal to N_c from Eq. (6) for the zero bias.

Although the mobility is very small, the change of quasi-Fermi level across the depletion region is assumed to be negligible under forward bias, since the tunneling through the interfacial layer constitutes the bottleneck for the current flow. This assumption on the flatness of the quasi-Fermi level is proved in Sec. V. It is considered that n_s is in thermal equilibrium with the bulk semiconductor. Thus the quasi-Fermi level in the depletion region coincides with the Fermi level E_{Fs} in the bulk, which is illustrated as extending to the interface in Figs. 1 and 2. Taking into account the change of barrier height due to applied bias by Eqs. (4) and (5), n_s becomes

$$n_s = N_c \exp\left(-\frac{q}{kT}(\phi_B - V)\right)$$

$$= N_c \exp\left(-\frac{q\phi_B^0}{kT}\right)\exp\left(-\frac{q\Delta V_D}{kT}\right)$$

$$= N_c \exp\left(-\frac{q\phi_B^0}{kT}\right)\exp\left[\frac{qV}{kT}\left(1-(1-\gamma)\frac{D_{sb}}{D_s}\right)\right]. \quad (7)$$

The forward current is given by Eqs. (6) and (7) to be

$$J = qP\left[n_s - N_c \exp\left(-\frac{q\phi_B}{kT}\right)\right]$$

$$= qPN_c \exp\left(-\frac{q\phi_B^0}{kT}\right)\exp\left[\frac{qV}{kT}\left(1-(1-\gamma)\frac{D_{sb}}{D_s}\right)\right]$$

$$\times\left[1-\exp\left(-\frac{qV}{kT}\right)\right]. \quad (8)$$

For $V \gtrsim 3kT/q$, Eq. (8) becomes

$$J = qPN_c \exp\left(-\frac{q\phi_B^0}{kT}\right)\exp\left(-\frac{q\Delta V_D}{kT}\right)$$

$$= qPN_c \exp\left(-\frac{q\phi_B^0}{kT}\right)\exp\left[\frac{qV}{kT}\left(1-(1-\gamma)\frac{D_{sb}}{D_s}\right)\right]. \quad (8a)$$

For the reverse bias, the signs of voltage, current, and electric field are changed to positive for convenience. The reverse current can be obtained as the carrier flow from the interface into the bulk by Eq. (6), since both n_s and $d\zeta/dx$ are involved in making up the carrier flow in reverse direction. The carrier concentration n_s is given by solving Eq. (6) to be

$$n_s = \frac{PN_c}{[P+\mu(d\zeta/dx)]}\exp\left(-\frac{q\phi_B}{kT}\right). \quad (9)$$

In thermal equilibrium with the interface states, n_s is

$$n_s = N_c \exp\left[-\frac{q}{kT}\left(\phi_B + \frac{D_{sb}}{D_s}V\right)\right]$$

$$= N_c \exp\left(-\frac{q\phi_B^0}{kT}\right)\exp\left(-\frac{qV}{kT}\frac{\gamma D_{sb}}{D_s}\right). \quad (10)$$

Equating Eqs. (9) and (10), we have

$$\exp\left(\frac{qV}{kT}\frac{D_{sb}}{D_s}\right) = 1 + \frac{\mu}{P}\frac{d\zeta}{dx}. \quad (11)$$

Since the carriers at the interface tend to flow into the bulk rather than to tunnel back to the metal under the reverse bias, Eq. (6) implies that $(\mu/P)d\zeta/dx$ is a large quantity compared to unity. Therefore, the current is given by

$$J = qn_s\mu\frac{d\zeta}{dx}$$

$$= qPN_c \exp\left(-\frac{q\phi_B^0}{kT}\right)\exp\left(\frac{qV}{kT}(1-\gamma)\frac{D_{sb}}{D_s}\right)$$

$$\times\left[1-\exp\left(-\frac{qV}{kT}\frac{D_{sb}}{D_s}\right)\right] \quad (12)$$

from Eqs. (10) and (11). For large reverse bias ($D_{sb}V/D_s \gtrsim 3kT/q$, J simply becomes

$$J = qPN_c \exp\left(-\frac{q\phi_B^0}{kT}\right)\exp\left(\frac{qV}{kT}(1-\gamma)\frac{D_{sb}}{D_s}\right)$$

$$= qPN_c \exp\left(-\frac{q\phi_B^0}{kT}\right)\exp\left(-\frac{q\Delta\phi_B}{kT}\right) \quad (12a)$$

by Eq. (4). Equation (12a) demonstrates that the reverse current does not show saturation but increases as an exponential function of the decrease of the barrier height due to the applied bias.

This bias dependence of the current is a result of multiplying two competing factors, n_s and $(d\zeta/dx)$, in Eq. (12). Although n_s decreases with reverse bias according to Eq. (10), $(d\zeta/dx)$ increases with reverse bias by a larger rate than n_s according to Eq. (11). It should be noted that if there is no decrease of the barrier height due to the applied bias, the saturation of reverse current results since the decreasing rate of n_s becomes larger than Eq. (10) and just cancels the increasing rate of $(d\zeta/dx)$ with reverse bias.

According to the thermionic emission theory, the J-V characteristics are expressed by[2]

$$J = AT^2 \exp(-q\phi_B/kT)[\exp(qV/kT) - 1]. \quad (13)$$

Here, A is called the Richardson constant. AT^2 is obtained from the energy distribution of electrons at the inner edge of the depletion region as well as the velocity of electrons surmounting the barrier to be[2]

$$AT^2 = \frac{4\pi q m^* k^2 T^2}{h^3}, \quad (14)$$

where m^* is the effective mass of the electron and h is the Planck's constant.

In the present analyses, the quantity corresponding to AT^2 is qPN_c in Eqs. (8a) and (12a) for either direction of current. For a low-mobility semiconductor such as a-Si:H, in which the mean free path of electrons is shorter than the mean distance between atomic sites from the standard transport theory, the thermal velocity is not an appropriate quantity to be defined.[10] However, if P is set equal to the thermal velocity of electrons,[2] $v_R = \sqrt{kT/2\pi m^*}$, times the transmission coefficient T_T of tunneling, qPN_c becomes

$$qPN_c = AT^2(P/\sqrt{kT/2\pi m^*}) = AT^2 T_T. \tag{15}$$

The present results are in accordance with the thermionic emission theory except for the factor T_T as for the magnitude of the current.

III. SAMPLE PREPARATION

The experimental samples have a substrate glass/first metal/a-Si:H/second metal structure. As the first metal, Cr was sputtered on an alkali-free glass. Undoped a-Si:H film was deposited on the substrate kept at 250 °C by plasma-enhanced chemical vapor deposition (CVD) to 3000 Å to about a 2 μm thickness. Before evaporating the second metal, the surface of the a-Si:H film was lightly etched with dilute HF solution. The metal evaporation was made on this a-Si:H film through a mask without heating the substrate. The electrode has an area 3 mm^2. As the second metal, Al, Cr, Ni-Cr, and Mo were used. These metals have nearly the same work functions[11] and no significant differences are observed in the experimental results. Gold was also used as the second metal which has a larger work function[11] than the above four kinds of metals. Experimental results of this diode give a larger barrier height than the above four kinds of diodes. From the observed J-V characteristics, the second metal contact with a-Si:H is the Schottky barrier in accordance with previous results.[7,12] In the following, the experimental results of samples with Ni-Cr as the second metal are reported.

To insure ohmic contact at the first metal contact, samples were prepared by depositing a several hundreds Å thick n^+-doped layer prior to the deposition of the undoped a-Si:H layer.[7,12] The J-V characteristics of these samples are qualitatively the same as those without the n^+ layer. The effect of the n^+ contacting layer is described in Sec. V. As for the thickness of the film, thick films are preferable for measurements of J-V characteristics under large forward bias. Thin films cannot withstand large forward bias because of small series resistance.

IV. RESULTS AND ANALYSES

A. Forward characteristics

The experimental J-V characteristics for the forward bias voltage at various temperatures between 30 and 150 °C are shown in Fig. 3. These curves differ considerably from the ideal characteristics and are qualitatively reproducible irrespective of samples. The data between 0.07 and 0.15 V are chosen for the following analyses because of $V \gtrsim 3kT/q$ and because they are free from series resistance effects.

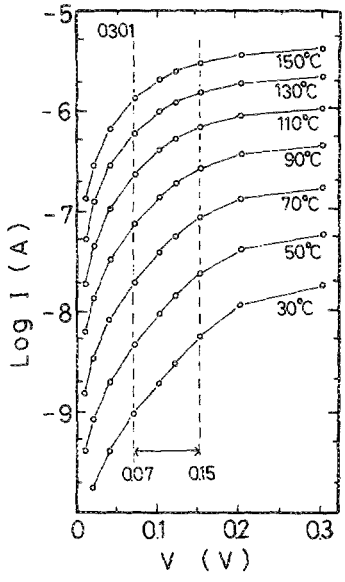

FIG. 3. I-V characteristics in forward direction at various temperatures. Data within the voltage range shown by the dashed lines (0.07–0.15 V) are used for analyses. The sample number is 0301.

To represent the experimental results for the forward bias, usually the ideality factor n is used; i.e.,

$$J = J_0 \exp(-q\phi_B^0/kT)\exp(qV/nkT), \tag{16}$$

where J_0 is a constant. By comparing Eqs. (5), (9), and (16), n is related to the quantities of the interfacial layer model by[5]

$$(1/n) = -(\Delta V_D/V) = 1 - (\Delta\phi_B/V), \tag{17}$$

and D_{sb}/D_s is expressed by

$$\frac{D_{sb}}{D_s} = \frac{n-1}{(1-\gamma)n}. \tag{18}$$

In Fig. 4, n is plotted against $1/T$ for each applied voltage and it increases with decreasing $1/T$ for higher applied voltage at higher temperatures. This result indicates that D_{sb} is determined by some thermally activated processes. Therefore, the population in the interface states under forward bias can be described by the Fermi level. It is increased by the electron capture from the conduction band and is decreased by release of the captured electrons as illustrated in Fig. 2. The capture rate is proportional to

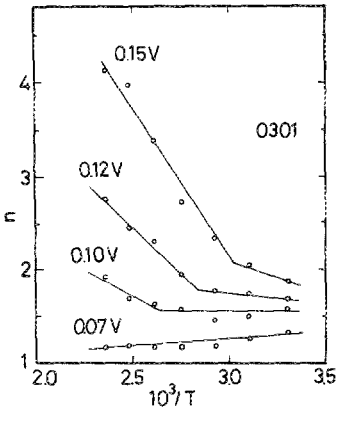

FIG. 4. Ideality factor n vs $1/T$ for various forward biases.

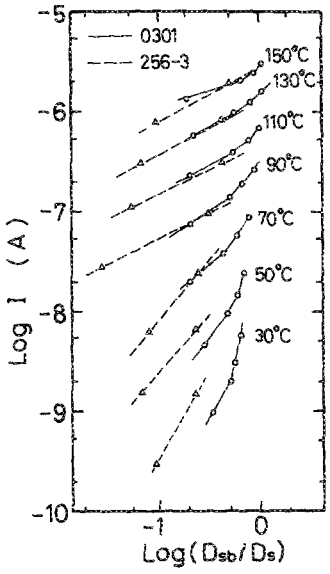

FIG. 5. D_{sb}/D_s vs forward current I for two samples at various temperatures. Sample numbers are 0301 and 256-3.

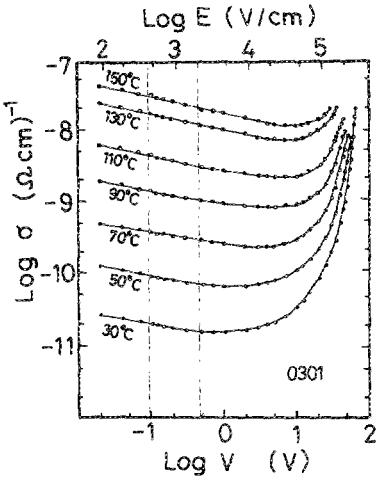

FIG. 6. Conductance σ vs reverse bias V characteristics at various temperatures. Data within the voltage range shown by the dashed lines (0.1–0.5 V) are used for analyses. Upper scale E indicates average applied field strength over the sample.

the carrier concentration at the top of the barrier. There are two possible electronic transitions for the release. One is a tunnel transition to the metal Fermi level through the interfacial layer and the other is a thermally activated release into the conduction band. While the transition probability of tunneling is considered to be nearly independent of temperature, the thermal release probability is expected to have an activation energy U close to the barrier height.

Therefore, D_{sb}/D_s is plotted against the forward current I, which is proportional to the carrier concentration n_s at the top of the barrier for each temperature for two samples in Fig. 5. The curves are similar in shape and are displaced to higher currents at higher temperatures. For each curve, D_{sb}/D_s is very small for low currents, increases with current, and converges to near unity at high currents. This result is understood as follows:

For the steady occupation of the interface states, the rates of capture and release are equal. This condition is represented by

$$Cn_s(D_s - D_{sb})V = [B^* + \nu \exp(-U/kT)]D_{sb}V. \quad (19)$$

The rate of capture is given by the left-hand side of Eq. (19), in which C is the capture coefficient and $(D_s - D_{sb})V$ is the number of vacant states available for capture. The rate of release is given by the right-hand side, in which B^* is the tunneling probability from the interface states to the metal, and ν is the attempt-to-escape frequency of the thermal release into the conduction band.

By solving Eq. (19), D_{sb}/D_s becomes

$$\frac{D_{sb}}{D_s} = \frac{Cn_s}{B^* + \nu \exp(-U/kT) + Cn_s}. \quad (20)$$

Since n_s is proportional to I, Eq. (20) represents the experimental results quite well. Depending on the magnitude of Cn_s relative to that of $[B^* + \nu \exp(-U/kT)]$, D_{sb}/D_s increases from a small value to near unity with increasing current. The experimental result that the larger current corresponds to the same D_{sb}/D_s value at higher temperatures implies that the thermal release probability is much larger than the tunneling probability B^*, which is nearly independent of temperature. However, the small D_{sb}/D_s value for the small current also implies the existence of small but finite B^*, because if $B^* = 0$ and the interface states communicate only with the conduction band, D_{sb}/D_s is considered to be near unity, independent of the current, and U is the same as the activation energy of n_s. The magnitude of B^* is discussed in Sec. V.

It should be noted that D_s is defined as the average state density between $q\phi_0$ and E_{Fm}, while D_{sb} is defined as the average occupied state density between E_{Fm} and E_{Fi}. Since the interface state density is a function of energy,[13] the maximum value of D_{sb}/D_s is not necessarily equal to unity. However, rapid variation of the density with energy is not likely and the proximity of the maximum D_{sb} to D_s is evidence to support the present analyses.

The above results indicate that tunnel transition probability of the captured electrons in the interface states is not large enough to disturb the thermal equilibrium distribution n_s with the bulk. D_{sb}/D_s increases with current from a small value to near unity.

B. Reverse characteristics

As for the reverse characteristics, the observed conductance σ is plotted against V in Fig. 6. Since the J-V characteristics are quite different from the ideal characteristics, it is better to plot σ rather than I for understanding what is occurring in the sample. All the curves are similar in shape and displaced parallel to the log σ axis with temperature. Data between 0.1 and 0.5 V are chosen for the following analyses because of $V \gtrsim 3kT/q$ and because they are free from generation of electron-hole pairs in the depletion region.

In Eq. (3), the induced charge VD_{sb} under the reverse bias is the opposite sign to the space charge under zero bias. Therefore, VD_{sb} represents the density of holes in the interface states, which are occupied by electrons under zero bias. Figure 7 is the energy-band diagram of the Schottky barrier under reverse bias illustrating the relation of $E_{Fi} = (D_{sb}/D_s)qV$ to the applied voltage V and others.

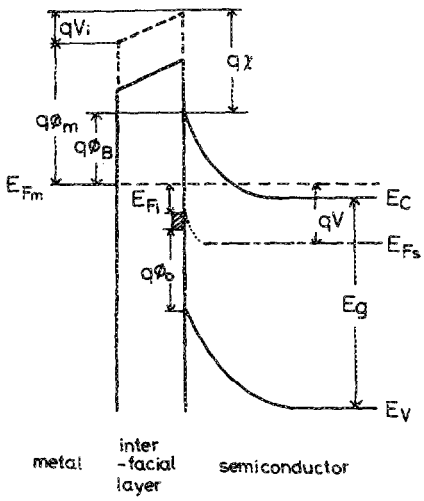

FIG. 7. Energy-band diagram of the Schottky barrier under reverse bias. The shaded area indicates the electron population in the interface states constituting space charge. The dotted line is the electron quasi-Fermi level. The dashed line in the interfacial layer is the vacuum level.

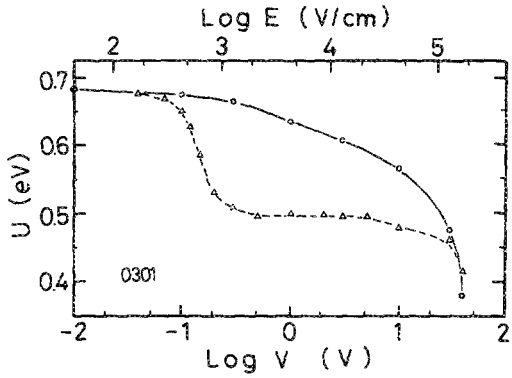

FIG. 9. Activation energies U vs applied voltage V for both forward current (triangles) and reverse current (circles). Upper scale E indicates average applied field strength over the sample.

The shaded area indicates the electron population in the interface states constituting the space charge. Here, the dotted line is the electron quasi-Fermi level $q\zeta$, which rises in the neighbor of the interface from E_{Fs} and coincides with E_{Fi} at the interface. The assumption in Sec. II B that n_s is in thermal equilibrium with E_{Fi} is considered to be a good approximation, since the tunnel transition probability B^* is small compared with other transition probabilities as demonstrated for the forward characteristics.

The analyses are made according to the equation

$$\ln\left(\frac{\sigma}{\sigma_0}\frac{qV}{kT}\right)=\frac{qV}{kT}(1-\gamma)\frac{D_{sb}}{D_s}-\ln\left(\frac{D_{sb}}{D_s}\right)_0, \qquad (21)$$

which is obtained from Eq. (12) and σ_0 and $(D_{sb}/D_s)_0$ stand for the values of σ and (D_{sb}/D_s) extrapolated to $V=0$, respectively. $(D_{sb}/D_s)_0$ is assumed to be 1 and this assumption becomes reasonable shortly. The experimental D_{sb}/D_s thus obtained is plotted in Fig. 8 against V. Since D_{sb}/D_s values are slightly dependent on temperature, the values at two temperatures are shown. In Fig. 8, D_{sb}/D_s decreases with increasing reverse bias V in an approximate proportionality to $1/\sqrt{V}$, and extrapolates to unity at roughly $V=kT/q$. This means that the barrier height decreases proportionally to $\sqrt{V}$ with applied voltage according to Eqs. (4) and (12a).

The above result is understood as follows: As discussed in Sec. II B, $d\zeta/dx$ increases approximately as an exponential function of reverse bias according to Eq. (11) and the total variation of ζ across the depletion region amounts to $(V-E_{Fi}/q)$. On the other hand, $E_{Fi}/q=D_{sb}V/D_s$ varies nearly proportionally to $\sqrt{V}$ with reverse bias. The ratio of the quasi-Fermi level drop at the interface to the total applied voltage, D_{sb}/D_s, decreases with increasing reverse bias. This ratio becomes a small fraction for large reverse bias. This is nearly the same situation as has been considered for a reverse-biased Schottky barrier without an interfacial layer.[1-3] Equations describing relations among ζ, V, and D_{sb}/D_s are complicated. However, there is no terms directly related to activated processes in these equations. Accordingly, it is reasonable that the observed temperature dependence of D_{sb}/D_s is very small compared with that of forward characteristics. The observed variation of D_{sb}/D_s being nearly proportional to $1/\sqrt{V}$ in the present sample is a very simple and interesting relation. Further studies are necessary to make the origin of this relation clear.

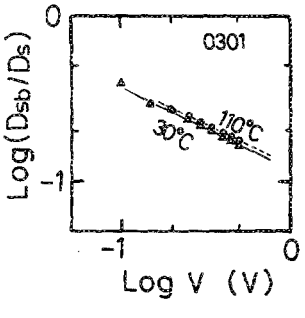

FIG. 8. D_{sb}/D_s vs reverse bias V at two temperatures.

C. Activation energies of current

The activation energies of current are a convenient measure of mechanisms which are limiting the current. Since the J-V characteristics for various temperatures are measured, the activation energies U of the current are obtained for both forward and reverse voltages. The results are plotted in Fig. 9 against the applied voltage. For low applied bias, the activation energy is 0.69 eV for both forward and reverse bias. This is the Schottky barrier height at zero bias.

With increasing forward bias up to about 0.2 V, the activation energy decreases to 0.50 eV. This activation energy is constant up to about 10 V. The activation energy gradually decreases from about 10 V and rapidly from about 30 V with increasing applied voltage. The initial decrease is due to a decrease of the diffusion potential, from 0.19 V to zero, in agreement with previous work.[14] The

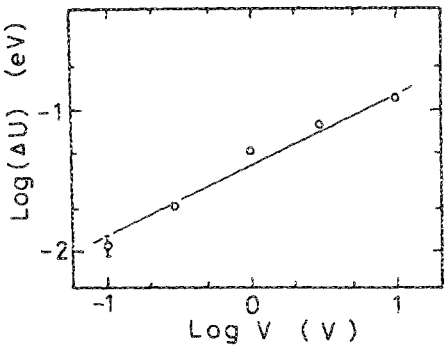

FIG. 10. Decrease of activation energy ΔU for reverse current against applied voltage V. The straight line shows the relation ΔU being proportional to $\sqrt{V}$. The vertical line indicates the range of uncertainty.

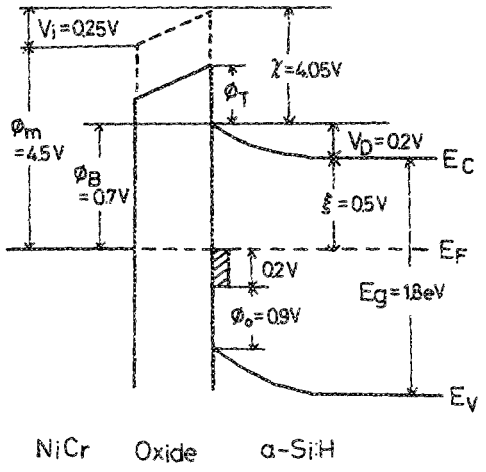

FIG. 11. Energy-band diagram of the Schottky barrier between Ni-Cr and a-Si:H with the interfacial layer under zero bias. The shaded area represents the electron population in the interface states constituting space charge. The dashed line for interfacial layer corresponds to vacuum level.

activation energy of 0.50 eV is considered to be the activation energy of the conductivity of undoped a-Si:H. Larger values than this have often been assigned to the activation energy of undoped a-Si:H, e.g., 0.6 eV by Spear *et al.*[15] The value of the activation energy depends on samples, but it has been pointed out to be difficult to remove the possible effects of contacts and surfaces for this high-resistance and thin-film semiconductor.[16] In the present study, these effects are absent.

It is considered that the gradual decrease in the forward direction is due to some electron injection, probably by generation current in the depletion region adjacent to the contact on the opposite side. The final decrease is due to filling up of the gap states by a space-charge-limited current.[17] A large injection of carriers is necessary for the space-charged-limited current to flow.

As for the activation energy of the reverse current, it is better to refer to the σ-V characteristics shown in Fig. 6. A gradual decrease is observed with increasing voltage to about 20 V, where a rapid decrease starts. The gradual decrease is considered to be a decrease $-\Delta\phi_B$ of the Schottky barrier height due to the applied voltage. Since the decrease of the barrier height is proportional to $\sqrt{V}$ for small reverse bias, as discussed in Sec. IV B, the decrease $-\Delta U$ of the activation energy is plotted against voltage in Fig. 10. The straight line in Fig. 10 is proportional to $\sqrt{V}$, and the observed data align along this line. Therefore, the variation of the observed activation energies for large applied voltages is consistent with the present analyses by the interfacial layer model. The absolute value of $\Delta\phi_B$ predicted by Eq. (4) from the value of D_{sh}/D_s in Fig. 8 is about twice as large as the decrease ΔU of the activation energy in Fig. 10. The former is obtained by analyzing the bias dependence of the current and the latter is obtained by analyzing the temperature dependence of the current. Such disagreement probably comes from the simplicity of the present analysis.

The rapid decrease in reverse direction is associated with the conductivity increase, i.e., the carrier injection probably due to the generation of hole-electron pairs in the depletion region of the reverse-biased Schottky barrier and the space-charge-limited current in the same way as for the forward bias. The behavior of this conductivity change is a little different from the forward characteristics, since the regions where the carriers are generated are on the opposite side depending on the direction of the applied bias.

Using the results of the above analyses, the energy-band diagram of the Schottky barrier between Ni-Cr and undoped a-Si:H in thermal equilibrium is drawn as shown in Fig. 11 .

V. DISCUSSION

For the J-V characteristics of undoped a-Si:H Schottky barriers, the departure from the ideal metal-semiconductor contact is quantitatively and consistently explained above by the interfacial layer model without taking other transport mechanisms and corrections into account. Since the present analyses use only D_{sh}/D_s as a variable concerning the interface states, no ambiguous quantity is introduced. While the present analyses are made in small voltage ranges where the J-V characteristics are dominated by the barrier itself on some simplifying assumptions, the intrinsic nature of the Schottky barrier is disclosed. The qualitative reproducibility of the characteristics is good for many samples measured. Quantitative differences arise in the dependence of the ideality factor on voltage and temperature shown in Fig. 4, when the opposite contact with metal is made on n^+-doped a-Si:H. However, the essential feature of the present analysis, i.e., dependence of D_{sh}/D_s on forward current and reverse voltage, is the same. The temperature dependence of the ideality factor was clearly seen in the undoped samples and it was a motivation for describing the population in the interface states by E_{Fr}. This is the reason why the experimental data of undoped samples are used in this report.

Among the assumptions, the most important is that the carrier density at the interface is in thermal equilibrium with the bulk, i.e., the quasi-Fermi level is flat throughout

the depletion region. Although it is very difficult to prove this assumption, estimations of the magnitudes of the related quantities are made in the following:

Since J is constant for a given forward voltage throughout the depletion region, the maximum of $d\zeta/dx$ appears at the position where the carrier density is minimum, i.e., at the interface by Eq. (6). Provided that the value of $d\zeta/dx$ at the interface is smaller than the average applied field V/d over the depletion region, the quasi-Fermi level can be considered to be flat across the depletion region. Since the carrier mobility is small and the mean free path is shorter than the mean atomic distance λ in a-Si:H as stated in Sec. II B, the rate of tunneling is better described by

$$Pn_s = Bn_s\lambda, \tag{22}$$

taking into account the electrons in the first atomic layer at the interface and B is the tunneling probability of a localized electron. Then the condition to be proved from Eq. (6) becomes

$$\frac{V}{d} > \left(\frac{d\zeta}{dx}\right)_{\max} = \frac{B\lambda}{\mu}. \tag{23}$$

B is considered to be represented by $B = a\exp(-b)$. The preexponential factor a is similar to that of the electron hopping probability in the impurity conduction,[18] in which the preexponential factor has a wide range of values and may be of the order of 10^{12} s^{-1}, which is compared with the optical phonon frequency of the order of 10^{13} s^{-1}. The exponent b is estimated to be equal to that of the tunneling probability of carriers for a rectangular barrier with an effective barrier height $q\phi_T$ and width δ[2]: i.e.,

$$b = \alpha_T \phi_T^{1/2}\delta, \tag{24}$$

where α_T approaches unity if the effective mass in the insulator equals the free-electron mass m_0 and if ϕ_T is in volts and δ in Å. The barrier height is the difference of electron affinities between the insulator and a-Si:H. The insulator is considered to be SiO_2, and χ is 1.0 eV for the thick SiO_2 film.[19] For a-Si:H, χ is 4.0 ± 0.1 eV.[7] However, the barrier height of 3 eV is too high to give a reasonable tunneling probability. Since the insulator is several atomic layers thick and not necessarily stoichiometric, its energy band may be different from that of thick SiO_2 film.[5] If ϕ_T is assumed to be 0.25 V, it leads to consistent results. Using $\delta = 10$ Å, B becomes 7×10^9 s^{-1}. With $\mu = 1.0$ cm^2/V s and $\lambda = 2\times10^{-8}$ cm, $(d\zeta/dx)_{\max}$ becomes 1.4×10^2 V/cm by Eq. (23). On the other hand, for $V = 0.1$ V and $d = 0.5\times10^{-4}$ cm, V/d becomes 2×10^3 V/cm, which is larger than the above value of $(d\zeta/dx)_{\max}$.

The value of $(d\zeta/dx)_{\max}$ depends strongly on ϕ_T. To assure the choice of ϕ_T, the absolute value of the forward current is calculated. A comparison of Eqs. (15) and (22) shows B is related to the transmission coefficient T_T of tunneling for the conducting electron by

$$T_T = B\lambda/v_R, \tag{25}$$

and T_T represents the current ratio of the present theory to the thermionic emission theory by Eq. (15). Putting $v_R = 2.7\times10^6$ cm/s for $m^* = m_0$, T_T becomes 5×10^{-5} by Eq. (25). On the other hand, the observed current density is 7×10^{-8} A/cm^2 for $V = 0.10$ V at room temperature. The theoretical current density by the thermionic emission theory for $\phi_B = 0.69$ V and $V = 0.10$ V is 1.5×10^{-3} A/cm^2. Therefore, the above T_T represents the current ratio satisfactorily. In the energy-band diagram, Fig. 11, $\phi_T = 0.25$ V is equal to the interfacial potential $V_i = (\phi_B + \chi) - \phi_m = 0.25$ V. Then, this value of ϕ_T is a mean value of the barrier height across the interfacial layer. Since this agreement indicates consistency among the adopted quantities, the present model is proved by the above estimation to represent quite well the actual Schottky barrier with an interfacial layer. Although δ is assumed here to be 10 Å, it is not unambiguous. The values of δ and ϕ_T are adjustable, keeping b constant by Eq. (24).

The tunnel transition from the interface states is discussed in Eq. (19). Here, the tunnel transition probability B^* is smaller than B, since the barrier height ϕ_T^* for the electrons in the interface states is larger than that for the electrons in the conduction band by the barrier height, i.e., $\phi_T^* = 0.94$ V. B^* is estimated to be much smaller than B, approximately by a factor of 10^{-2} according to Eq. (24). The ratio of the tunneling current J_i from the interface states to the tunneling current J of conducting carriers can be estimated by

$$\frac{J_i}{J} = \frac{B^* D_{sb} V}{Bn_s\lambda} = \frac{B^*}{B\lambda}\,\frac{D_s C V}{[B^* + \nu\exp(-U/kT) + CN_c\exp(-q\phi_B/kT)\exp(qV/kT)]} \tag{26}$$

using Eqs. (7), (19), (20), and (22). The maximum value of J_i/J appears for small applied bias when B^* is larger than

$$[\nu\exp(-U/kT) + CN_c\exp(-q\phi_B/kT)\exp(qV/kT)]$$

in the denominator of Eq. (26) and it is

$$J_i/J = CD_sV/B\lambda. \tag{27}$$

Equation (27) means that the maximum J_i/J is equal to the ratio of capture probability to tunneling probability for the conducting electrons at the interface. However, the observed dependence of D_{sb}/D_s on temperature and current shown in Fig. 5 implies that B^* is smaller than

$$[\nu\exp(-U/kT) + CN_c\exp(-q\phi_B/kT)\exp(qV/kT)].$$

For this condition, Eq. (26) indicates that J_i increases lin-

early with bias, while J increases exponentially with bias. Thus, J_i/J is ordinarily very small compared to unity.

As for the decrease of barrier height under the reverse bias, the image force lowering has been considered.[1,2,20] By the present theory, the decrease can be explained as described in Sec. II. The decrease of barrier height by the interfacial layer model is larger than and has a different bias dependence from the image force lowering of the barrier height. The reason why the image force lowering is not taken into account in the potential consideration of Eq. (4) for the Schottky barrier with an interfacial layer is as follows:

The electric field inducing the image force for conducting carriers close to the interface is considered to be shielded from the metal by the space charge in the interface states. The position of the potential maximum in the image force lowering model exists up to several tens of Å from the interface depending on both the applied field and the built-in potential of the semiconductor. However, the tunneling through the interfacial layer is not so deep into the semiconductor. Therefore, it is difficult to consider that the image force lowering is effective in the present case.

As described above, both the assumptions in the present model and the results obtained by comparing experiment and theory are reasonable. Therefore, the present model is considered to represent the actual a-Si:H Schottky barrier quite well. This model is expected to be also applicable to other Schottky barriers. Since the ideality factor and soft reverse characteristics cannot usually be explained by the ordinary theory, it is interesting to investigate an applicability of the present theory to these Schottky barriers.

VI. CONCLUSIONS

The following conclusions are obtained by the present study. A new theory of nonideal J-V characteristics of the Schottky barrier with an interfacial layer is developed. This theory is based on the following model.

(1) The nonideal characteristics are due to changes of population in the interface states under applied bias, which induce changes of the barrier height. This population is represented by the Fermi level of the interface states.

(2) The J-V characteristics are obtained from the flow of carriers into and out of the interface. Under forward bias, the carrier concentration n_s at the interface is in thermal equilibrium with the bulk. Under reverse bias, both n_s and the population of the interface states, which are in local thermal equilibrium, decrease due to the applied field.

The observed nonideal J-V characteristics of the undoped a-Si:H Schottky barrier are consistent with this model. The following results are obtained by comparing theory with experiment.

(3) At low forward bias, the Fermi level of the interface states is significantly low compared with the Fermi level in the bulk. However, the former approaches to the latter with increasing current.

(4) Under reverse bias, the induced potential across the interfacial layer decreases the barrier height with the applied voltage V proportionally to $\sqrt{V}$ in the present sample.

(5) For the electrons in the interface states, the tunneling probability to and from the metal is small compared with the capture and release probabilities through the conduction band.

Since these results are reasonable, this interfacial layer model is concluded to represent actual Schottky barriers quite well. Further investigations are needed to clarify the interesting behavior of the Fermi level in the interface states under applied bias. It is interesting to investigate an applicability of the present theory to other Schottky barriers.

ACKNOWLEDGMENTS

The authors thank Professor Y. Uemura for his critical reading of the manuscript. This work was supported in part by Toshiba Corporation.

[1] E. H. Rhoderick, *Metal-Semiconductor Contacts* (Clarendon, Oxford, 1978).
[2] S. M. Sze, *Physics of Semiconductor Devices* (Wiley, New York, 1981).
[3] M. S. Tyagi, in *Metal-Semiconductor Schottky Barrier Junctions and Their Applications*, edited by B. L. Sharma (Plenum, New York, 1984), p. 1.
[4] A. M. Cowley and S. M. Sze, J. Appl. Phys. **36**, 3212 (1965).
[5] H. C. Card and E. H. Rhoderick, J. Phys. D **4**, 1589 (1971).
[6] Zs. J. Horvath, J. Appl. Phys. **63**, 976 (1988).
[7] J. Kanicki, C. M. Ransom, W. Bauhofer, T. I. Chappel, and B. A. Scott, J. Non-Cryst. Solids **66**, 51 (1984).
[8] H. Fritzsche, in *Semiconductors and Semimetals*, edited by J. I. Pankove (Academic, New York, 1984), Vol. 21, Pt. C, p. 309.
[9] J. P. Ponpon and B. Bourdon, Solid State Electron. **25**, 875 (1982).
[10] J. Dresner, in *Semiconductors and Semimetals*, edited by J. I. Pankove (Academic, New York, 1984), Vol. 21, Pt. C, p. 193.
[11] *American Institute of Physics Handbook*, 3rd Ed. (McGraw-Hill, New York, 1982), Sec. 9.
[12] J. Kanicki, Appl. Phys. Lett. **53**, 1943 (1988).
[13] S. Kar and W. E. Dahlke, Solid State Electron. **15**, 221 (1972).
[14] R. A. Street, Phys. Rev. B **27**, 4924 (1983).
[15] W. E. Spear and P. G. LeComber, Philos. Mag. **33**, 935 (1976).
[16] H. Fritzche, Solar Energy Mater. **3**, 447 (1980).
[17] J. W. Orton and M. J. Powell, Philos. Mag. B **50**, 11 (1984).
[18] N. F. Mott and E. A. Davis, *Electronic Processes in Noncrystalline Materials* (Clarendon, Oxford, 1979).
[19] R. Williams, Phys. Rev. **140**, A569 (1965).
[20] S. M. Sze, C. R. Crowell, and D. Kahng, J. Appl. Phys. **35**, 2534 (1964).